A STUDY OF TROPICAL THIN CIRRUS CLOUDS WITH SUPERVISED LEARNING

Sharon Rodier [(1)], Yongxiang Hu [(2)], Mark Vaughan [(2)]

[(1)] SSAI, MS 4757, Langley Research Center, Hampton VA, USA 23681; E-mail: sharon.d.rodier@nasa.gov
[(2)] NASA, MS 475, Langley Research Center, Hampton VA, USA 23681; E-mail: Yongxiang.Hu-1@nasa.gov
[(2)] NASA, MS 475, Langley Research Center, Hampton VA, USA 23681; E-mail: mark.a.vaughan@nasa.gov

ABSTRACT

Recent studies using general regression neural networks have shown that by mapping the collocated brightness temperatures from the CALIPSO Imaging Infrared Radiometer (IIR) [1] and the sea surface temperatures form Aqua's Advanced Microwave Scanning Radiometer (AMSR-E) [2] to the optical depths derived from the CALIPSO lidar [3], and then applying the trained network to the combination of passive sensor parameters alone, we can successfully retrieve the optical depths of previously undetected thin cirrus cloud embedded in the passive sensor measurements. In this paper, we describe our approach for using a supervised neural network to derive correlations between coincident active and passive measurements from the A-Train instruments. After briefly recounting the motivation for attempting the retrieval, we describe our methodology for training the network using the CALIPSO lidar optical depths. We subsequently validate this methodology using two test scenarios, and discuss future applications designed to increase the information derived from passive measurements. Our preliminary validation studies show that when applying this method we can expect reliable retrievals of optical depths as small as ~0.1, with a success rate of ~95%.

1. INTRODUCTION

Accurate knowledge of the temporal frequency and spatial extent of optically thin cirrus is crucial to climate feedback analysis. Current global warming theory asserts that when the atmospheric concentration of CO_2 increases, the outgoing longwave radiation at non-window wavelengths (outside of the 8-12micron range) is reduced. If the Earth's net radiative balance is to remain stable, ground temperatures must rise in response, thereby increasing thermal emission to space. Current Global Climate Models (GCM) differ significantly in terms of cloud feedback [4]. One possible response of the cloud-climate feedback process is an increase in the global occurrence of thin cirrus clouds, driven by the increase in longwave cooling in the stratosphere. Exacerbating the difficulty of assessing the situation has been the fact that passive remote sensing instruments cannot reliably detect cirrus clouds with optical depths less than ~0.3, because these clouds do not reflect enough sunlight to create a sufficient contrast with the Earth's surface. Now, however, the presence of thin cirrus can for the first time be accurately detected and systematically monitored by the combination of active and passive sensors onboard the CALIPSO satellite. Nevertheless, the data record is still quite limited, as CALIPSO has been in orbit for only 20 months. We have, therefore, initiated a multi-platform data fusion study to establish a methodology for extending the limited set of CALIPSO measurements to the existing 30-year record of passive remote sensing data, and thus improve our understanding of cloud feedback mechanisms.

Our initial study was limited to nighttime data from the first 10 days in April 2007. We applied a general regression neural network (GRNN) to collocated samples of sea surface temperature (SST) reported by AMSR-E, brightness temperatures (BT) from the CALIPSO IIR, and optical depths (OD) derived from the CALIPSO lidar measurements. The results revealed an accurate mapping of the optical depths derived from the active sensors to the brightness temperatures computed from the passive sensor measurements. In testing the trained network using the combination of passive sensor parameters, we found that optical depths as small as 0.1 could be reliably retrieved. Similar results are obtained in the larger follow-on study reported here, in which we apply the same methodology to all of the nighttime data acquired during December 2007.

2. DATA SELECTION AND PREPARATION

Instruments aboard the A-train constellation of Earth observing satellites provided the measurements used in this study. Observations from the CALIOP lidar aboard CALIPSO were combined with passive imagery from the CALIPSO IIR and AMSR-E. The IIR is a nadir-viewing, non-scanning imager having a 64 km by 64 km swath with a pixel size of 1 km. The CALIOP beam is nominally aligned with the center pixel of the IIR image. Over ocean, AMSR-E provides sea surface temperatures from beneath most types of cloud cover, supplementing infrared-based measurements of SST that are restricted to cloud-free areas. The processed SST data is mapped to 0.25-degree grid.

Optical depths at a 5km horizontal resolution were retrieved from the CALIPSO Level II data products. Because solar background significantly reduces the

signal-to-noise ratios of daytime CALIOP measurements, we have restricted our initial investigations to nighttime data only. The IIR 8.55, 10.6, and 12.05 micron radiances were converted to brightness temperature then averaged along-track to a 5km resolution around the center pixel that was coincidental with the lidar footprint. The collocated SST measurements were converted to degrees Kelvin.

Three hundred and ninety six nighttime orbit segments from December 2007 were searched for CALIPSO measurements that met the following criteria: single-layer transparent (i.e., not opaque) clouds with tops above 6-km, situated over ocean between 30° N and 30° S, having valid, collocated measurements of both SST from AMSR-E and BT from the IIR. This produced 16,517 records. These records were configured to created a collection of data vectors that best represented the optical properties of the cloud structures identified during the selection process. The IIR's choice of spectral bands was specifically designed for the study of cirrus clouds, which allows utilization of the classic split window technique along with the 10.6-micron channel. Finally, by subtracting the emission from the sea surface from the 10.6-micron brightness temperature, we get the true brightness temperature of the remaining cloud or body. The parameters are shown in Table 1**.** Available data is split into two sets, a training set and a test set.

Table 1: GRNN Data Vector Parameters

Input Parameters:	
1.	SST – BT 10.6 micron
2.	BT10.6 micron - BT 12.05 micron
3.	BT 10.6 micron – BT 8.65 micron
4.	BT 10.6 micron
Training Parameters	
1.	Cloud Optical Depth – Calipso
2.	Cloud Optical Depth – Passive
Output Parameters	
1.	Cloud Optical Depth

2. GENERAL REGRESSION NEURAL NETWORK

GRNNs belong to a class of supervised neural networks that perform regression where the target variable is continuous. [6] In supervised learning, the network is trained on a training set consisting of vector pairs. One vector is applied to the input of the network; the other is used as a "target" representing the desired output. Training is accomplished by adjusting the network weights so as to minimize the difference between the desired and actual network outputs. The GRNN uses a radial basis function (RBF) to map data vector inputs to the best matching outputs. [7] GRNNs are comprised of two layers of artificial neurons. The first layer, the "Radial Basis Layer", consists of neurons which process data vectors in three consecutive steps. The initial weights are calculated by simply transposing the data vectors from the training set. Next, a Euclidean distance is calculated between an input vector and these weights. Finally, the values are rescaled by the selected input spreading factor. The second "Linear Transfer Layer" consists of neurons with a linear transfer function. Each data vector is solved to minimize the sum-squared error between the output of the first layer and the desired output.

One advantage of the GRNN approach is simplicity. In addition to having an extremely fast learning rate, being very accurate, and relatively insensitive to outliers, a GRNN has only one tunable parameter, the spreading factor *h*. As *h* increases, the radial basis function decreases in width. The network will respond with the target vector being associated with the nearest designated input vector. As the spreading factor becomes smaller, the radial basis function increases in width. Several neurons may then respond to an input vector, and thus as the radial basis function gets wider and wider, more neurons contribute to the average, resulting in a smoother model function.

Given a training set and an independent test set, a GRNN is trained by choosing the spreading factor to obtain the best precision in the estimations. The GRNN structure is illustrated in Figure 1.

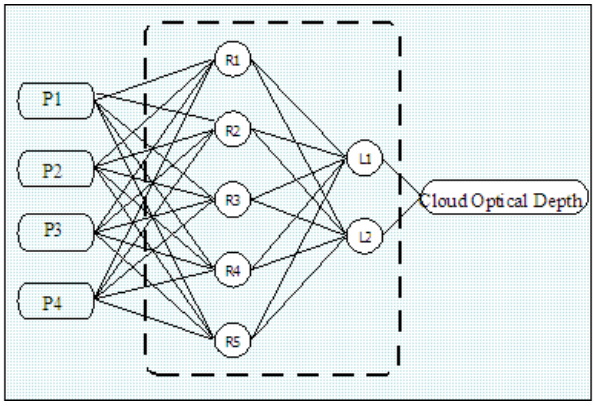

Figure 1 Layout of GRNN used in this study. P1-P4 represent the input parameters from Table 1. R1-R5 represnt the radial bais layer. L1-L2 represent the Linear Transfer Layer. The Cloud Optical Depth is the final output of the GRNN

2.1 Initialization and Training of the GRNN

A random set of 6000 input vectors was selected from the 16,517 data pool to perform the initial training and

calibration. During the calibration process, the input training set is fed to the GRNN for multiple iterations, altering the spreading function value before each run. After each execution the Mean Squared Error (MSE) between the estimated optical depth and the CALIPSO derived optical depths is calculated. The spreading function producing the smallest MSE is chosen for the remaining training and testing of the data set. Table 2 documents the MSE values for each run. A spreading function of 1 was found to be the best match for this data set.

Table 2: Spreading Function Mean Squared Error

Spreading Function	.5	1	1.2
MSE	0.0515	0.0026	0.0029

Once the spreading function is selected, the GRNN requires a single iteration to produce the trained net. A quick comparison between the derived optical depths and those generated by the GRNN is performed. Figure illustrates a snap shot of the first 100 samples of the trained net.

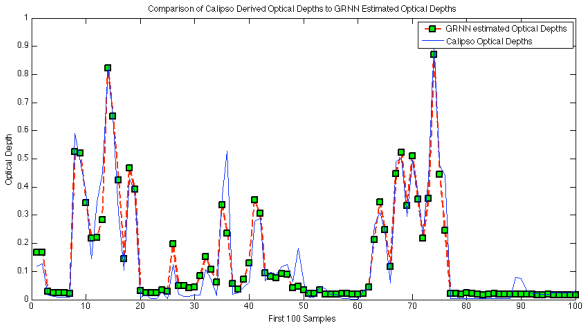

Figure 2. Comparison of CALIPSO derived optical depths (blue) to GRNN estimated optical depths (red dashed, green box), for the first 100-samples**.**

Complete analysis of the 6000-vector training set is required to verify a valid training set before continuing the testing phase.

2.2 Testing and Evaluation of the GRNN

Analysis of the GRNN performance is accomplished using established statistical methods for Neural Net evaluation [5]: The Root Mean Squared Error (RMSE), Mean Absolute Error (MAE) and the Correlation Coefficient are calculated after each execution.

Evaluation of the net output for the randomly selected 6000 vectors training set indicates a successful duplication of the optical depth values during our training cycle. The log-log plot in Figure 3 shows a strong correlation (R = .9593) between the two data sets for optical depths to approximately ~0.1.

Table 3 documents the complete statistical evaluation from the training cycle.

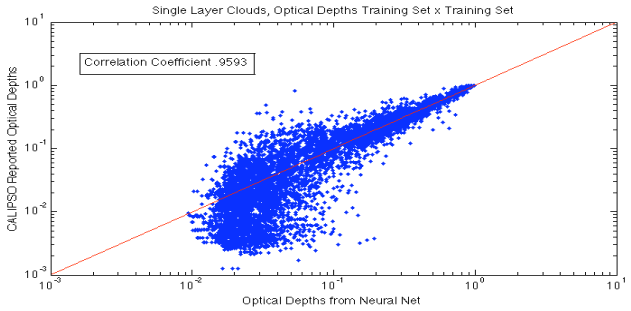

Figure 3 A log-log plot of the training results for GRNN estimated optical depths to the CALIPSO derived optical depths

The next phase of testing consists of applying the trained net to two sets of test data. The first is a random set of 6000 vectors selected from the remaining 10,517-vector data pool, and to the second is all vectors available in the test data set. First we perform what is considered a traditional test case. This is where the quantity of training set vectors is equal to or greater than the number of test data vectors. In this scenario all possible data characteristics should be well represented by the training data set. The second test case uses a training data set that contains a much smaller quantity of data vectors than will subsequently be used in the test data set. This procedure simulates training a GRNN with the available CALIPSO data and then applying it to the vast quantity of historical passive sensor measurements from multiple platforms.

One iteration of the network will map the input of the test data set to the best matching estimated optical depth created during the training phase. Figure 4 shows a second log-log comparison with a strong correlation (R= .950) for the final testing cycle. Statistical evaluations for the testing cycles are documented in Table 3.

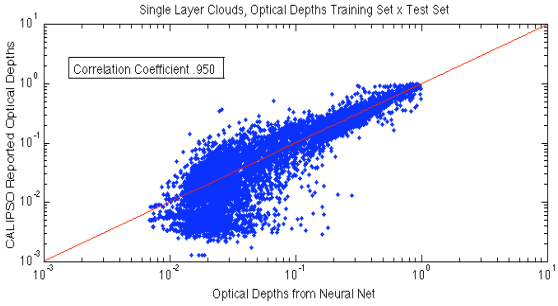

Figure 4 Log-log plot of testing results for the GRNN estimated optical depths compared to the CALIPSO derived optical depths 6000 vector training set x 10000 vector test set.

Table 3 Statistical Evalusation of GRNN Training and Testing Cycles

Net Cycle data set size	Spreading Function	MAE	RMSE	Correlation Coefficient
Training 6000	1	0.0326	0.0513	.9593
Testing 6000	1	0.0352	0.0564	.951
Testing 10000	1	0.0354	0.0566	.950

3. SUMMARY

During our preliminary studies (April 2007) we tested a methodology for constructing a supervised neural network to derive cirrus cloud optical depths both from the on-going A-Train data stream and from the historical database of passive sensor measurements. The preliminary results indicated that the GRNN could be trained to estimate the optical depths of thin cirrus clouds embedded in the passive sensor measurements when these measurements were mapped to the collocated CALIPSO lidar optical depths. When we subsequently apply the trained network to a test set of passive sensor parameters alone, we extract cirrus cloud optical depths as small as ~0.1 with a success rate of 95%. To further validate this methodology, we expanded the quantity of data being used for the training and test data sets, initialized the GRNN, and re-executed. December 2007 was selected, data vectors were prepared, testing and training was repeated. The new training cycle produced estimated optical depth values that had a high correlation (R= ~.96) with the actual CALIPSO optical depths and a small RMSE of 0.0513. The trained net was applied to the two expanded test data sets. Again the network produced estimated optical depth values with a high correlation with the actual values. In both cases we had minimum of ~.95 correlation with a RMSE no greater than 0.056. In our judgment, the success rate for this methodology is very good. Given an appropriate amount of training data, this approach appears promising for extending the knowledge gained from the CALIPSO nadir measurements to the full swath of collocated passive sensor measurements of SST and brightness temperature. It is conceivable that a sufficiently well-trained GRNN could eventually provide estimates of thin cirrus optical depths using the full historical database of pre-CALIPSO measurements. However, when training neural networks it is critically important that each element of the training set is sufficiently represented over the data range for that element. In our specific case, this means we must sample enough combined "cirrus cloud scenes" to correctly estimate the optical depth for each scene type. For further investigations it will be very beneficial to have multiple months, and eventually years, of collocated data to serve as the training set. This will allow us to meet our objective of enhancing and extracting additional information form other passive data products such as MODIS

GRNNs are exceptionally easy to train, producing accurate and reliable results with the minimum number of inputs. The only draw back to the GRNN architecture can be system memory requirements for large data sets. Field-programmable gate array (FPGA) hardware provides a reliable alternative to this problem [8].

REFERENCES

[1] O.Chomette, A. Garnier, J. Pelon , A. Lifermann (2003) Retrieval of cloud emissivity and particle size in the frame of the CALIPSO mission. Geoscience and Remote Sensing Symposium, 2003 IGARSS'02 Proceedings. 2003 IEEE International

[2] F. Wentz T. Meissner Algorithm Theoretical Basis Document (ATBD), Version 2, AMSR Ocean algorithm, Remote Sensing Systems

[3] D. M. Winker, et al., The CALIPSO mission: spaceborne lidar for observation of aerosols and clouds, *Proc. SPIE*, Vol. 4893, pp.1–11, 2003

[4] Cess, R. D., et al. (1996), Cloud feedback in atmospheric general circulation models: An update, *J. Geophys. Res.*, *101*(D8), 12,791–12,794.

[5] Balaguer, E., Soria, E., Carrasco, J.L., del Valle, S., 2001. Prediction if surface ozone concentrations 24 h in advance using neural networks. In: Advanced in Neural Networks and Applications. World Scientific and Engineering Press, EEUU, pp. 212– 214.

[6] P. Wasserman, Advanced Methods in Neural Computing, Van Nostrand-Reinhold, New York, 1993.

[7] Specht, D.E., G general Regression Neural Network, IEEE Trans. Neural Networks, No 5, Vol 2, 1991, pp 568-892

[8] Lazaro, Arias et al. (2004) An Implementation of a General Regression Neural Network on FPGA with direct Matlab Link IEEE International Conference on Industrial Technology (ICIT)